

$\Lambda\Lambda$ - ΞN - $\Sigma\Sigma$ coupling in ${}^6_{\Lambda\Lambda}\text{He}$ with the Nijmegen soft-core potentials

Taiichi Yamada

Laboratory of Physics, Kanto Gakuin University, Yokohama 236-8501, Japan

(Dated: September 29, 2018)

Abstract

The $\Lambda\Lambda$ - ΞN - $\Sigma\Sigma$ coupling in ${}^6_{\Lambda\Lambda}\text{He}$ is studied with the $[\alpha+\Lambda+\Lambda] + [\alpha+\Xi+N] + [\alpha+\Sigma+\Sigma]$ model, where the α particle is assumed as a frozen core. We use the Nijmegen soft-core potentials, NSC97e and NSC97f, for the valence baryon-baryon part, and the phenomenological potentials for the $\alpha-B$ parts ($B=N, \Lambda, \Xi$ and Σ). We find that the calculated $\Delta B_{\Lambda\Lambda}$ of ${}^6_{\Lambda\Lambda}\text{He}$ for NSC97e and NSC97f are, respectively, 0.6 and 0.4 MeV in the full coupled-channel calculation, the results of which are about half in comparison with the experimental data, $\Delta B_{\Lambda\Lambda}^{exp} = 1.01 \pm 0.20^{+0.18}_{-0.11}$ MeV. Characteristics of the $S = -2$ sector in the NSC97 potentials are discussed in detail.

PACS numbers: 21.80.+a, 13.75.Ev, 21.45.+v

I. INTRODUCTION

The study of strangeness $S = -2$ nuclei is an entrance to multistrangeness hadronic systems and provides unified understanding of YN and YY interactions among baryon octet. The $S = -2$ nuclei serve important information on the YN and YY interactions, because free-space baryon-baryon scattering experiments in $S = -2$ sector are difficult to be performed at the present stage. Since the $\Lambda\Lambda$ - ΞN - $\Sigma\Sigma$ coupling including the H -dibaryon state is induced, there might exist exotic nuclei with $S = -2$ such as H -nuclear states and/or hyperon-mixed nuclear states among baryon octet.

A recent discovery of ${}_{\Lambda\Lambda}^6\text{He}$ in the KEK-E373 experiment [1], which is called as *NAGARA*, has provided a great impact in hypernuclear physics. The importance is due to the ambiguity-free identification of the hypernucleus and the high quality experimental $\Lambda\Lambda$ binding energy $B_{\Lambda\Lambda} = 7.25 \pm 0.19 \pm_{0.11}^{0.18}$ MeV [1], which leads to a smaller $\Lambda\Lambda$ bond energy, $\Delta B_{\Lambda\Lambda} = B_{\Lambda\Lambda}({}_{\Lambda\Lambda}^6\text{He}) - 2B_{\Lambda}({}_{\Lambda}^5\text{He}) = 1.01 \pm 0.20 \pm_{0.11}^{0.18}$ MeV, indicating that the $\Lambda\Lambda$ interaction is more weakly attractive than that reported over 30 years ago [2]. Although it is identified as double- Λ nucleus, we cannot exclude a possibility of H -nuclear state or hyperon-mixed state among baryon octet, because we know only the binding energy. The data of the NAGARA event indicates four possibilities on the YN and YY interactions as follows; 1) weakly attractive $\Lambda\Lambda$ interaction with weak $\Lambda\Lambda$ - ΞN - $\Sigma\Sigma$ coupling effect, 2) almost zero or weak repulsive $\Lambda\Lambda$ interaction with moderate $\Lambda\Lambda$ - ΞN - $\Sigma\Sigma$ coupling effect, 3) repulsive $\Lambda\Lambda$ interaction with strong $\Lambda\Lambda$ - ΞN - $\Sigma\Sigma$ coupling effect, and 4) $\Lambda\Lambda$ - ΞN - $\Sigma\Sigma$ coupling so strong as to produce a weakly-bound or resonant H -dibaryon state. Forthcoming experiments for $S = -2$ nuclei as well as the H -dibaryon state will disclose characteristics of the YN and YY interactions together with the structure of $S = -2$ nuclei and hyperon mixing.

After the discovery of the NAGARA event [1], several authors have discussed the strength of the $\Lambda\Lambda$ interaction and structure of ${}_{\Lambda\Lambda}^6\text{He}$ as well as ${}_{\Lambda\Lambda}^4\text{H}$ and ${}_{\Lambda\Lambda}^5\text{H}$ - ${}_{\Lambda\Lambda}^5\text{He}$. The binding energies of ${}_{\Lambda\Lambda}^6\text{He}$ and ${}_{\Lambda\Lambda}^4\text{H}$ were studied with the Fadeev-Yakubovsky approach [3, 4, 5], where they used the phenomenological $\Lambda\Lambda$ interaction (central-type) which reproduces the low energy parameters of the Nijmegen soft-core potential [6]. The systematic three- and four-body calculations of p -shell double- Λ nuclei [7] were performed with the phenomenological $\Lambda\Lambda$ potential reproducing the NAGARA data. On the other hand, the Brueckner theory approach was applied to studying the $\Lambda\Lambda$ bond energy and rearrangement effect in ${}_{\Lambda\Lambda}^6\text{He}$. [8,

9, 10] The Ξ component as well as the $\Lambda\Lambda$ bond energy was discussed in ${}^5_{\Lambda\Lambda}\text{H}$ and ${}^5_{\Lambda\Lambda}\text{He}$ [8, 11]. The 6-body calculation within the framework of the stochastic variational method has been performed with phenomenological (central-type) baryon-baryon interactions. [12]

The purpose of the present paper is to study the $\Lambda\Lambda$ - ΞN - $\Sigma\Sigma$ coupling effect in ${}^6_{\Lambda\Lambda}\text{He}$ with the realistic baryon-baryon potential for the two-valence-baryon part. We use the $[\alpha+\Lambda+\Lambda] + [\alpha+\Xi+N] + [\alpha+\Sigma+\Sigma]$ model, where the α particle is assumed as a frozen core. The Nijmegen soft-core potentials, NSC97e and NSC97f [6], are directly applied to the valence baryon-baryon interactions. Phenomenological potentials are used for the α - B parts ($B=N, \Lambda, \Xi$ and Σ). The formulation is almost the same as one in our previous paper [13], where structure of light $S = -2$ nuclei and hyperon mixing were discussed. The Pauli blocking effect of the valence nucleon in the $\alpha+\Xi+N$ channel is taken into account properly. We will discuss the calculated energies and coupled-channel effects in ${}^6_{\Lambda\Lambda}\text{He}$ together with the characteristics of the Nijmegen potentials.

II. FORMULATION

The total wave function of ${}^6_{\Lambda\Lambda}\text{He}$ with total angular momentum J is given as

$$\Phi = \Phi_{\Lambda\Lambda} + \Phi_{\Xi N} + \Phi_{\Sigma\Sigma}, \quad (1)$$

$$\Phi_{\Lambda\Lambda} = \sum_{\beta=1}^2 \sum_{LS} \mathcal{A}_{\Lambda\Lambda} \left[\Phi_L^{(\Lambda\Lambda)\beta}(\mathbf{r}_\beta, \mathbf{R}_\beta) \left[\chi_{1/2}(\Lambda)\chi_{1/2}(\Lambda) \right]_{S,I=0} \right]_J, \quad (2)$$

$$\Phi_{\Xi N} = \sum_{\beta=1}^3 \sum_{LS} \left[\Phi_L^{(\Xi N)\beta}(\mathbf{r}_\beta, \mathbf{R}_\beta) \left[\chi_{1/2}(\Xi)\chi_{1/2}(N) \right]_{S,I=0} \right]_J, \quad (3)$$

$$\Phi_{\Sigma\Sigma} = \sum_{\beta=1}^2 \sum_{LS} \mathcal{A}_{\Sigma\Sigma} \left[\Phi_L^{(\Sigma\Sigma)\beta}(\mathbf{r}_\beta, \mathbf{R}_\beta) \left[\chi_{1/2}(\Sigma)\chi_{1/2}(\Sigma) \right]_{S,I=0} \right]_J, \quad (4)$$

where β denotes the Jacobian coordinate system (see Fig. 2 in Ref. [13]), and $\Phi_L^{(\beta)}$ and χ 's represent, respectively, the wave function of the spatial part with total orbital angular momentum L and the spin-isospin functions for the valence baryons coupled to total spin S and isospin I . In the $\alpha+\Lambda+\Lambda$ ($\alpha+\Sigma+\Sigma$) channel, the antisymmetrization operator $\mathcal{A}_{\Lambda\Lambda}$ ($\mathcal{A}_{\Sigma\Sigma}$) is needed for the two Λ (Σ) particles. Therefore, it is enough to take the two Jacobian coordinate systems for the $\alpha+\Lambda+\Lambda$ ($\alpha+\Sigma+\Sigma$) channel.

The wave function of the spatial part $\Phi_L(\mathbf{r}, \mathbf{R})$ in Eqs. (2), (3) and (4) is expanded in terms of the Gaussian basis, which is known to be suited for describing both the short-range

correlation and long-range tail behavior [14],

$$\Phi_{LM}(\mathbf{r}, \mathbf{R}) = \sum_{\ell_r, \ell_R} \sum_{n_r, n_R} C_{n_r, \ell_r, n_R, \ell_R}^L [\varphi_{\ell_r}(\mathbf{r}, \nu_{n_r}) \varphi_{\ell_R}(\mathbf{R}, \nu_{n_R})]_{LM}, \quad (5)$$

$$\varphi_{\ell m}(\mathbf{r}, \nu) = N_\ell(\nu) r^\ell \exp(-\nu r^2) Y_{\ell m}(\hat{\mathbf{r}}), \quad (6)$$

where $N_\ell(\nu)$ is the normalization factor. The Gaussian parameter ν is taken to be of geometrical progression,

$$\nu_n = 1/b_n^2, \quad b_n = b_{min} a^{n-1}, \quad n = 1 \sim n_{max}. \quad (7)$$

It is noted that the prescription is found to be very useful in optimizing the ranges with a small number of free parameters together with high accuracy [14].

The total Hamiltonian within the framework of the $[\alpha + \Lambda + \Lambda] + [\alpha + \Xi + N] + [\alpha + \Sigma + \Sigma]$ model is given as

$$H = \delta_{cc'} [T_c + V_{\alpha B_1}(\mathbf{r}_1) + V_{\alpha B_2}(\mathbf{r}_2) + \Delta M_c] + v_{cc'}(\mathbf{r}_3) + \delta_{c2} V_{Pauli}, \quad (8)$$

where c denotes the channel; $c = 1$ for $\alpha + \Lambda + \Lambda$, $c = 2$ for $\alpha + \Xi + N$ and $c = 3$ for $\alpha + \Sigma + \Sigma$. T_c and $V_{\alpha B}$ present, respectively, the kinetic energy operator and potential between the α particle and valence baryon B , and $v_{cc'}$ denotes the interaction between the two valence baryons. In the present study, the baryon-channel coupling is assumed to come only from $v_{cc'}$. The mass difference matrix (diagonal and constant) ΔM_c is introduced to give the threshold-energy differences among the three channels, $\Delta M_1=0$ MeV, $\Delta M_2=28$ MeV and $\Delta M_3=160$ MeV. The Pauli principle between the α cluster and valence nucleon in the $\alpha + \Xi + N$ channel is taken into account with the orthogonality condition model (OCM) [15]. The Pauli-blocking operator V_{Pauli} [16] is represented as

$$V_{Pauli} = \lim_{\lambda \rightarrow \infty} \lambda | \varphi_{0s}(\mathbf{r}_{\alpha N}) \rangle \langle \varphi_{0s}(\mathbf{r}'_{\alpha N}) |, \quad (9)$$

which removes the Pauli forbidden state φ_{0s} between the α cluster and valence nucleon in the core+ Ξ + N three-body system. The configuration of α cluster is assumed here to be of simple $(0s)^4$ -shell-model type.

The potential between the α cluster and valence hyperon $V_{\alpha Y}$ for $Y = \Lambda, \Xi$ and Σ is obtained by folding the effective hyperon-nucleon (YN) interaction with the density of the α particle and adjusting their strength so as to reproduce the experimental binding energy

for the ground state of the $\alpha+Y$ system with use of the $\alpha+Y$ potential model. As for the effective hyperon-nucleon (YN), we use the YNG-ND interaction [17]. It is known that the YNG-ND ΛN interaction reproduces nicely the Λ binding energy of ${}^5_\Lambda\text{He}$ as well as other light Λ hypernuclei, and the ΞN interaction is consistent with the recent experimental data on ${}^{12}_{\Xi}\text{B}$ obtained by the ${}^{12}\text{C}(K^-, K^+)$ reaction [18]. The YNG-ND ΣN interaction is also consistent with the experimental data of ${}^4_\Sigma\text{He}$ [19]. Concerning the density distribution for the α particle, we use the harmonic-oscillator-type one obtained by the electron scattering experiment [20]. The α - Ξ potential obtained is so weak as to give the Ξ binding energy as small as 0.01 MeV for the system, while the α - Σ potential produces no bound states. As for the α - N potential, we use the Kanada-Kaneko potential [21], constructed with the resonating group method (RGM) based on the microscopic theory, which reproduces precisely the scattering phase shifts for the $p_{3/2}$, $p_{1/2}$, and $s_{1/2}$ partial waves etc. at low energies. The potential is local with parity dependent central and spin-orbit terms. It is noted that we need to take into account the Pauli-blocking operator in Eq. (9) when applying the potential to the $\alpha+N$ ($\alpha + \Xi + N$) system.

The interaction between the two valence baryons $v_{cc'}$ in Eq. (8) is given as

$$v(r) = v^{(0)}(r) + v^{(\sigma)}(r)(\boldsymbol{\sigma}_1 \cdot \boldsymbol{\sigma}_2) + v^{(ten)}(r)S_{12} + v^{(LS)}(r)\mathbf{L} \cdot \mathbf{S} + v^{(ALS)}(r)\mathbf{L} \cdot \mathbf{S}^- + v^{(QLS)}(r)Q_{12} - [\nabla^2\phi(r) + \phi(r)\nabla^2], \quad (10)$$

where the notation is self-explanatory. In the present paper, we use the Nijmegen soft-core potentials, NSC97e and NSC97f [6], for the interaction between the two valence baryons.

The equation of motion is derived from the Rayleigh-Ritz variational method,

$$\delta [\langle \Phi | E - H | \Phi \rangle] = 0. \quad (11)$$

Solving the equation numerically, we obtain the eigenenergies of the Hamiltonian given in Eq. (8) and expansion coefficients of the wave function C 's in Eq. (5).

For the later discussion, it is instructive here to formulate the equation of motion for the two baryon system with $S = -2$ and spin-isospin zero. The Hamiltonian of the system is given as

$$h = \delta_{cc'} \left[-\frac{\hbar^2}{2\mu_c} \nabla^2 + \Delta M_c \right] + v_{cc'}(\mathbf{r}), \quad (12)$$

where $v_{cc'}$ is the baryon-baryon interaction in Eq. (10). The total wave function with orbital angular momentum ℓ is presented as

$$\phi = \phi_{\Lambda\Lambda} + \phi_{\Xi N} + \phi_{\Sigma\Sigma}, \quad (13)$$

$$\phi_{\Lambda\Lambda} = \phi_{\ell}^{(\Lambda\Lambda)}(\mathbf{r}) \left[\chi_{1/2}(\Lambda)\chi_{1/2}(\Lambda) \right]_{S=I=0}, \quad (14)$$

$$\phi_{\Xi N} = \phi_{\ell}^{(\Xi N)}(\mathbf{r}) \left[\chi_{1/2}(\Xi)\chi_{1/2}(N) \right]_{S=I=0}, \quad (15)$$

$$\phi_{\Sigma\Sigma} = \phi_{\ell}^{(\Sigma\Sigma)}(\mathbf{r}) \left[\chi_{1/2}(\Sigma)\chi_{1/2}(\Sigma) \right]_{S=I=0}, \quad (16)$$

where \mathbf{r} denotes the relative coordinate between the two-baryon system. The wave function of the spatial part $\phi_{\ell}(\mathbf{r})$ is expanded into the Gaussian basis φ_{ℓ} in Eq. (6),

$$\phi_{\ell}(\mathbf{r}) = \sum_n c_{n\ell} \varphi_{\ell}(\mathbf{r}, \nu_n). \quad (17)$$

The equation motion is derived from the variational method, $\delta [\langle \phi | \epsilon - h | \phi \rangle] = 0$, and corresponds to that in Eq. (11) under the condition of choosing only the Jacobian coordinate with $\beta = 1$ in Eqs. (2)~(4) and setting to $|\mathbf{R}_1| \rightarrow \infty$, where \mathbf{R}_1 denotes the relative coordinate of the $\alpha - (BB)$ part with $(BB) = (\Lambda\Lambda)$, (ΞN) and $(\Sigma\Sigma)$.

III. RESULTS AND DISCUSSION

A. 1S_0 state of two-baryon system with $S = -2$ and $I = 0$

It is instructive, first of all, to study the characteristics of the NSC97e and NSC97f potentials by solving the Schrödinger equation for the two-baryon system with $S = -2$ and isospin $I = 0$ with the Hamiltonian in Eq. (12). The calculated energies of the 1S_0 state, $E_{\Lambda\Lambda}$ ($= -B_{\Lambda\Lambda}$), with respect to the $\Lambda + \Lambda$ threshold are listed in Table I for various coupled-channel cases.

In the single $\Lambda\Lambda$ channel case, both the NSC97e and NSC97f potentials give no bound states as well as in the $\Lambda\Lambda$ and ΞN coupled-channel case. This result suggests that the coupling effect of the $\Lambda\Lambda$ - ΞN conversion potential is weak in both the potentials. Figure 1 shows the radial behaviors of $v_{\Lambda\Lambda-\Lambda\Lambda}(r)$, $v_{\Xi N-\Xi N}(r)$ and $v_{\Lambda\Lambda-\Xi N}(r)$ for NSC97e, where the momentum-dependent term in Eq. (10) is not included. The behaviors for NSC97f are almost the same as those for NSC97e. Although the coupling potential, $v_{\Lambda\Lambda-\Xi N}$, is strong in the short-range region, the coupling effect becomes weak due to the following reasons: Both the

$v_{\Lambda\Lambda-\Lambda\Lambda}$ and $v_{\Xi N-\Xi N}$ potentials have very strongly repulsive part in the short-range region and very weakly attractive one in the outer region, the characteristics of which make the amplitude of the relative wave function between the two Λ particles (as well as between the Ξ and N particles) smaller, so that the coupling matrix element becomes very small. Consequently, the coupling effect is weak in the $\Lambda\Lambda-\Xi N$ channel system.

In case of the $\Lambda\Lambda$ and $\Sigma\Sigma$ coupled-channel problem with NSC97e, however, we find that a bound state with $B_{\Lambda\Lambda} \sim 21$ MeV [22], where the channel components are $P_{\Lambda\Lambda} = 48\%$ and $P_{\Sigma\Sigma} = 52\%$ (see Table I). The result is surprising for us. The mechanism of producing such a bound state is follows: Figure 2 shows the radial behaviors of $v_{\Lambda\Lambda-\Lambda\Lambda}(r)$, $v_{\Sigma\Sigma-\Sigma\Sigma}(r)$ and $v_{\Lambda\Lambda-\Sigma\Sigma}(r)$ for NSC97e, where the momentum-dependent term in Eq. (10) is not included. The attractive (repulsive) behavior of $v_{\Sigma\Sigma-\Sigma\Sigma}$ ($v_{\Lambda\Lambda-\Lambda\Lambda}$) in the short-range region makes the energy of the $\Sigma\Sigma$ -channel ($\Lambda\Lambda$ -channel) state push down (push up). Both the energies, then, are almost degenerate in energy or the energy of the $\Sigma\Sigma$ channel is slightly smaller than that of the $\Lambda\Lambda$ channel. Reflecting the very strong coupling potential $v_{\Lambda\Lambda-\Sigma\Sigma}$ as shown in Fig. 2, then, the bound state appears in the short-range region. Although the above-mentioned explanation is a little bit schematic, the bound state is produced dynamically in the short-range region by solving the $\Lambda\Lambda$ and $\Sigma\Sigma$ coupled-channel problem in which the momentum-dependent term is switched on. On the other hand, in case of NSC97f, we could not find such a bound state in NSC97e (see Table I). The reasons are follows: Although the radial behavior of the coupling potential $v_{\Lambda\Lambda-\Sigma\Sigma}$ in NSC97f is almost the same as that in NSC97e, we found significantly quantitative differences of the diagonal potentials, $v_{\Sigma\Sigma-\Sigma\Sigma}$ and $v_{\Lambda\Lambda-\Lambda\Lambda}$, between NSC97e and 97f: The strength of the attraction (the repulsion) of $v_{\Sigma\Sigma-\Sigma\Sigma}$ ($v_{\Lambda\Lambda-\Lambda\Lambda}$) in NSC97f decreases (increases) by about $50 \sim 70$ % (by about 25 %) in the short-range region in comparison with NSC97e. The NSC97f potential, thus, has no ability to produce the situation like NSC97e, that the $\Sigma\Sigma$ - and $\Lambda\Lambda$ -channel states are almost degenerate in energy as discussed above, so that there is no bound state in the $\Lambda\Lambda$ - $\Sigma\Sigma$ channel system in NSC97f. The strong coupling effect with the $\Sigma\Sigma$ channel in NSC97f, however, can be seen in the ΞN - $\Sigma\Sigma$ channel which has a bound state with the binding energy $B_{\Lambda\Lambda}(= B_{\Xi N} - 28) \sim 82$ MeV (see Table I). Such a bound state appears also in NSC97e, but its binding energy is $B_{\Xi N} \sim 24$ MeV. We observe considerable quantitative differences of the binding energies of the two-baryon systems between NSC97e and 97f. Although the existence of the bound states in the two-channel problems seems to be strange, it is related

to a deeply bound state in the $\Lambda\Lambda$ - ΞN - $\Sigma\Sigma$ channel, the details of which will be discussed below.

Switching on the $\Lambda\Lambda$ - ΞN - $\Sigma\Sigma$ coupling, we find an extremely deeply bound state with the binding energy of $B_{\Lambda\Lambda}(=-E_{\Lambda\Lambda})=1475$ (1624) MeV for NSC97e (NSC97f), where the channel components are $P_{\Lambda\Lambda}=26.6$ (23.9) %, $P_{\Xi N}=31.1$ (32.1) % and $P_{\Sigma\Sigma}=42.4$ (44.0) % [22]. The appearance of the bound states astonishes us. It is noted that the momentum-dependent term in Eq. (10) is taken into account in the calculation. Although the calculated binding energies depend slightly on the choice of the Gaussian size parameters in Eq. (17) because of a singularity of the Nijmegen potentials at origin ($r = 0$) [22], the qualitative characteristics of the deeply bound state do not change very much. The radial wave function of the deeply bound state in the full coupled-channel case for NSC97e is illustrated in Fig. 3. The behavior of the wave function shows that the bound state is localized at $r \leq 0.5$ fm. From the channel components for the state (see Table I) and relative phases among the three channels (see Fig. 1), the deeply bound state obtained has a flavor-SU(3)- $\{8s\}$ -like character, $|8s\rangle = \sqrt{1/5}|\Lambda\Lambda\rangle + \sqrt{1/5}|\Xi N\rangle + \sqrt{3/5}|\Sigma\Sigma\rangle$. It is interesting, here, to study the effect of the momentum-dependent (MD) term on the binding energy and channel components of the deeply bound state. The calculated binding energy without MD is as large as $B_{\Lambda\Lambda}=2088$ (2374) MeV for NSC97e (97f), and thus, we found that the repulsive effect of MD is as large as about $600 \sim 700$ MeV, whose repulsive character can be inferred from the definition [see Eq. (10)]. On the other hand, the resultant channel components without the MD term are almost the same as those with it. The results, thus, indicate that the deeply bound state is not produced by only the MD term.

In order to study the mechanism of appearing the deeply bound state, the effective potential defined in Ref. [23] is calculated for the flavor-SU(3)- $\{8s\}$ state, the result of which is illustrated in Fig. 4 together with the flavor-SU(3)- $\{27\}$ potential for reference. In the calculation, the momentum-dependent (MD) term in Eq. (10) is explicitly taken into account. Although the flavor-SU(3)- $\{27\}$ potential behaves normally, we find a strong attraction in the short-range region for the flavor-SU(3)- $\{8s\}$ potential which produces the flavor-SU(3)- $\{8s\}$ -like deeply bound state in the NSC97e potential. The results for NSC97f are almost the same as those for NSC97e. In case without the MD term, the radial behavior of the flavor-SU(3)- $\{27\}$ potential is qualitatively similar to that with the MD term, but the strength of the attraction in the short-range region for the former is much larger than

that for the latter. Thus, the origin of the deeply bound state comes mainly from the fact that the bare terms without the MD term in Eq. (10) are designed to have much strong attraction in the flavor-SU(3)- $\{8s\}$ channel, the strength of which is so large as to overcome the repulsive effect originating from the MD term.

According to the quark-cluster model, one Pauli-forbidden state, a flavor-SU(3)- $\{8s\}$ state with the quark shell-model $(0s)^6$ configuration, appears in the 1S_0 two-baryon system with $S = -2$ and $I = 0$ [24]. The deeply bound states in NSC97e and NSC97f, thus, might be regarded as playing a Pauli-forbidden-state-like role in the potentials, although we don't know any reasons of why such a bound state is incorporated in the Nijmegen OBEP framework. It is remarked that the existence of the deeply bound states does not affect to the calculated results of the low-energy scattering parameters of NSC97e and NSC97f [6], because of the binding energy as large as $1500 \sim 1600$ MeV.

In this paper, we call the deeply bound states observed here as *pseudo bound states*, and impose the following condition on the wave function: physical states should be orthogonal to the pseudo bound states, when the NSC97 potentials are used in theoretical calculations. Since the 0_2^+ state obtained in the $\Lambda\Lambda$ - ΞN - $\Sigma\Sigma$ coupled-channel calculation in Table I is orthogonal to the pseudo bound state (0_1^+), the 0_2^+ state is interpreted as a physical state. The calculated results with the single channel problems and the two-channel problems in Table I, thus, lose physical meanings because their wave functions are not orthogonal to the *pseudo bound states*. We should note that the orthogonal condition does not give any influence to the results of the scattering length and effective range of NSC97e and NSC97f [6].

Careful treatments are needed to perform the structure calculation of ${}^6_{\Lambda\Lambda}\text{He}$, where the total wave function should not contain any component of the pseudo bound state. In the present framework, we can easily remove the pseudo-bound-state component from the total wave function in Eq. (1) by introducing the following exclusion operator in the total Hamiltonian in Eq. (8),

$$V_{PBS} = \lim_{|\lambda'| \rightarrow \infty} \lambda' | \varphi_{PBS}(\mathbf{r}_{BB}) \rangle \langle \varphi_{PBS}(\mathbf{r}'_{BB}) |, \quad (18)$$

where $\varphi_{PBS}(\mathbf{r}_{BB})$ is the pseudo bound state of the two-baryon system with the flavor-SU(3)- $\{8s\}$ -like character as mentioned above and \mathbf{r}_{BB} denotes the relative coordinate between the two baryons. The results of ${}^6_{\Lambda\Lambda}\text{He}$ will be presented in the next subsection (Sec. IIIB).

B. $\Lambda\Lambda$ - ΞN - $\Sigma\Sigma$ coupling in ${}^6_{\Lambda\Lambda}\text{He}$

Table II shows the full $\Lambda\Lambda$ - ΞN - $\Sigma\Sigma$ coupled-channel results of ${}^6_{\Lambda\Lambda}\text{He}$ with the exclusion operator V_{PBS} in Eq. (18) which removes the pseudo-bound-state component from the total wave function of ${}^6_{\Lambda\Lambda}\text{He}$. The calculated $\Delta B_{\Lambda\Lambda}$ of ${}^6_{\Lambda\Lambda}\text{He}$ is 0.61 (0.36) MeV for NSC97e (NSC97f), the value of which is about half in comparison with the experimental data, $\Delta B_{\Lambda\Lambda}^{exp} = 1.01 \pm 0.20^{+0.18}_{-0.11}$ MeV. The $\Lambda\Lambda$, ΞN and $\Sigma\Sigma$ components are, respectively, $P_{\Lambda\Lambda}=99.77$ (99.81) %, $P_{\Xi N}=0.21$ (0.18) % and $P_{\Sigma\Sigma}=0.01$ (0.01) % for NSC97e (NSC97f). The results indicate that the hyperon mixing effect is very small in the ground state of ${}^6_{\Lambda\Lambda}\text{He}$. Although the Nijmegen potentials have a singularity at the origin as mentioned in Sec. IIIA, we found that the effect to the calculated binding energy is less than 0.02 MeV because we used the exclusion operator V_{PBS} .

Here, it is instructive to discuss the calculated results of ${}^6_{\Lambda\Lambda}\text{He}$ for various coupled-channel cases without the exclusion operator V_{PBS} , although we have to remind that only the results of the full coupled-channel calculations with V_{PBS} are *physical* in the present paper as discussed in Sec. IIIA. The results are shown in Table II.

First let us see the results of only the $\Lambda\Lambda$ channel switching off the couplings with the ΞN and $\Sigma\Sigma$ channels. The calculated $\Delta B_{\Lambda\Lambda}$ of ${}^6_{\Lambda\Lambda}\text{He}$ is as small as 0.33 and 0.09 MeV, respectively, for NSC97e and NSC97f. In case of the $\alpha+\Lambda+\Lambda$ and $\alpha+\Xi+N$ coupled-channel problem, we find that $\Delta B_{\Lambda\Lambda}^{cal}$ is 1.36 (0.56) MeV for NSC97e (NSC97f), where the respective ΞN -channel components are as small as 0.55 (0.21) %. Switching on the full $\Lambda\Lambda$ - ΞN - $\Sigma\Sigma$ coupling, we obtain a deeply bound state of ${}^6_{\Lambda\Lambda}\text{He}$, 0_1^+ , with the flavor-SU(3)- $\{8s\}$ -like character for both the NSC97e and NSC97f potentials (see Table II). This is due to the fact that the two-baryon system ($\Lambda\Lambda$ - ΞN - $\Sigma\Sigma$) with $S = -2$ and $I = 0$ has a deeply bound state with the flavor-SU(3)- $\{8s\}$ -like character as discussed in Sec. IIIA. The reason of why the $\Delta B_{\Lambda\Lambda}$ values of 0_1^+ in Table II are smaller than those in the two-baryon system in Table I is ascribed mainly to the Pauli-blocking effect for the $\alpha + \Xi + N$ channel. The deeply bound state (0_1^+) of ${}^6_{\Lambda\Lambda}\text{He}$, thus, corresponds to a pseudo bound state or an unphysical state in the present study, and the second 0^+ state corresponds to a candidate of the physical state, although the state may have some component of the pseudo bound state of the two-valence-baryon system. The calculated $\Delta B_{\Lambda\Lambda}$ of the 0_2^+ state is 0.61 (0.36) MeV for NSC97e (NSC97f) in Table II. The values as well as the channel components are exactly the same

as those with the exclusion operator V_{PBS} . The reason is due to the fact that the binding energy of the pseudo bound state of the two-baryon system with $S = -2$ and $I = 0$ is as large as $B_{\Lambda\Lambda} = 1500 \sim 1600$ MeV, and therefore, the existence of the pseudo bound state gives almost no effect to the 0_2^+ state of ${}^6_{\Lambda\Lambda}\text{He}$. Comparing the energies of the 0_2^+ state in the full coupled-channel problem with those of the $\alpha+\Lambda+\Lambda$ and $\alpha+\Xi+N$ coupled-channel one, we observe that the $\Delta B_{\Lambda\Lambda}^{cal}$ value becomes smaller due to the $\Sigma\Sigma$ -channel coupling. Although it seems that the reduction suggests a repulsive effect of the $\Sigma\Sigma$ channel, the origin of the reduction is due to the existence of the pseudo bound state.

From the above results together with those in Sec. IIIA, we learn that the theoretical discussion on the binding energy of $S = -2$ nuclei without the $\Lambda\Lambda$ - ΞN - $\Sigma\Sigma$ coupling has no definite sense, because of the existence of the pseudo bound state in the NSC97e and NSC97f potentials. The pseudo bound state comes only from the full-channel calculation and is not produced in the single or two-channel problems. In the present framework, the component of the pseudo bound state is removed from the total wave function of ${}^6_{\Lambda\Lambda}\text{He}$ with the exclusion operator in the full coupled-channel calculation. The existence of the pseudo bound state, thus, enforces us to discuss only the full-channel problem, and it is not adequate to compare directly the results of the single-channel and two-channel calculations with those of the full-channel one.

It is interesting to see the effects of the binding energy and channel components of ${}^6_{\Lambda\Lambda}\text{He}$ on the choice of α - B potentials (B denotes baryon). The calculated results are discussed, hereafter, in the three-channel coupled problem including V_{PBS} [Eq. (18)] with NSC97e for the following four cases; 1) using the folding-type α - N potential [13], 2) neglecting the Pauli-blocking operator in Eq. (12), 3) neglecting the α - Ξ potential in the present study and 4) using the strongly repulsive α - Σ potential suggested in the experimental analysis of the ${}^{28}\text{Si}(\pi^-, K^+)$ reaction [25].

First we study the effect on the choice of the α - N potential. Although the Kanada-Kaneko (KK) potential was used in the present study, it is instructive to apply the folding potential which had used in the previous our paper [13]. It is derived from the folding procedure of the effective NN interaction, HNY [26], with the density of the α particle. The calculated results are follows: $\Delta B_{\Lambda\Lambda}=0.60$ MeV, $P_{\Lambda\Lambda}=99.79$ %, $P_{\Xi N}=0.19$ % and $P_{\Sigma\Sigma}=0.01$ %. They are almost the same as those with the KK potential (see Table II). We found, thus, that the calculated results do not depend on the details of the α - N potentials very much, because of

the ΞN component as small as 0.2 % in ${}^6_{\Lambda\Lambda}\text{He}$. Secondly, the effect of imposing the Pauli-blocking operator in Eq. (9) for the α - N system is investigated by dropping it out of the structure calculation for ${}^6_{\Lambda\Lambda}\text{He}$. In that case, both the Ξ particle and valence nucleon (N) can be in S orbit and the nucleon is bound by 12 MeV with respect to the $\alpha+n$ threshold for the KK potential. We expect that the ΞN component is enhanced. The results are follows: $\Delta B_{\Lambda\Lambda}=0.81$ MeV, $P_{\Lambda\Lambda} = 99.40$ %, $P_{\Xi N} = 0.58$ % and $P_{\Sigma\Sigma} = 0.02$ %. We see that the component of the ΞN channel without the Pauli-blocking operator is about three times larger than that with the operator (see Table II), although the energy gain is as small as about 0.2 MeV. This result encourages us to expect that the mass $A = 5$ system with $S = -2$ has the ΞN component larger than the present $A = 6$ system, because the former has no Pauli-blocking effect in the Ξ channel [8, 11].

Thirdly, the effect on the α - Ξ potential is investigated. In the present study, we used the folding potential derived from folding the YNG-ND ΞN interaction with the density of the α particle, which gives the Ξ -particle binding energy as small as $B_{\Xi}=0.01$ MeV for the $\alpha+\Xi$ system. Although the ΞN interaction is consistent with the recent experimental data on ${}^{12}_{\Xi}\text{B}$ produced in the ${}^{12}\text{C}(K^-, K^+)$ reaction, it is interesting to study what happens if the weak α - Ξ potential is neglected. The results are follows: $\Delta B_{\Lambda\Lambda}=0.60$ MeV, $P_{\Lambda\Lambda} = 99.79$ %, $P_{\Xi N} = 0.20$ % and $P_{\Sigma\Sigma} = 0.01$ %. They are almost the same as those with switching on the α - Ξ potential (see Table II). Thus, the effect from the α - Ξ potential is very weak in the ground state of ${}^6_{\Lambda\Lambda}\text{He}$, reflecting the very small component of the ΞN channel.

Finally, we study the effect on the α - Σ potential. The folding-type α - Σ potential was applied in Table I, where we used the YNG-ND ΣN interaction which is consistent with the experimental data of ${}^4_{\Sigma}\text{He}$. The α - Σ potential has a weak repulsive character. The recent experimental data on the ${}^{28}\text{Si}(\pi^-, K^+)$ reaction [25], however, suggested that a strongly repulsive Σ -nucleus potential is needed to reproduce the observed spectrum within the framework of DWIA. The real part of the phenomenological potential is of the Woods-Saxon (WS) type, $U(r) = U_0/\{1 + \exp[(r - c)/z]\}$, with $U_0=150$ MeV, $c = 1.1 \times (A - 1)^{1/3}$ fm and $z = 0.67$ fm [25]. It is interesting to investigate what happens if we use such a strong repulsive WS-type potential in ${}^6_{\Lambda\Lambda}\text{He}$. The results with V_{PBS} in Eq. (18) are follows: $\Delta B_{\Lambda\Lambda}=0.59$ MeV, $P_{\Lambda\Lambda} = 99.78$ %, $P_{\Xi N} = 0.21$ % and $P_{\Sigma\Sigma} = 0.01$ %. They are almost the same as those in Table II. The reason is due to the extremely small $\Sigma\Sigma$ component ($P_{\Sigma\Sigma} = 0.01$ %) in the ground state of ${}^6_{\Lambda\Lambda}\text{He}$ (see Table II). Some effects, however, were found in the pseudo-bound

state (PBS) of ${}^6_{\Lambda\Lambda}\text{He}$ in the calculation without V_{PBS} : $\Delta B_{\Lambda\Lambda}=1460$ MeV, $P_{\Lambda\Lambda} = 26.54$ %, $P_{\Xi N} = 30.86$ % and $P_{\Sigma\Sigma} = 42.60$ %. Comparing with the results in Table II, the binding energy decreases by about 7 MeV reflecting the repulsive character of the WS-type potential. The results indicate that the WS-type α - Σ potential is not so strongly repulsive as to suppress the PBS. The reason of why the potential does not suppress the PBS is given as follows: The PBS in ${}^6_{\Lambda\Lambda}\text{He}$ has a main structure of $\alpha + "BB"$, where $"BB"$ denotes the PBS in the two-baryon system with $S = -2$ with $B_{\Lambda\Lambda}=1475$ MeV. The main part of the binding energy in ${}^6_{\Lambda\Lambda}\text{He(PBS)}$, thus, comes from the interaction energy between the two valence baryons. This means that the contribution from the α - B potentials is not so large in comparison with that from the intra valence-baryon interactions. In addition, the effect of the WS-type repulsive α - Σ potential is weakened in ${}^6_{\Lambda\Lambda}\text{He(PBS)}$ because the $\Sigma\Sigma$ component is only about 40 %. Consequently, the binding energy of PBS in ${}^6_{\Lambda\Lambda}\text{He}$ is not changed drastically even though we use the repulsive WS-type α - Σ potential.

IV. SUMMARY

The $\Lambda\Lambda$ - ΞN - $\Sigma\Sigma$ coupling in ${}^6_{\Lambda\Lambda}\text{He}$ was investigated with the $[\alpha + \Lambda + \Lambda] + [\alpha + \Xi + N] + [\alpha + \Sigma + \Sigma]$ model, where the α particle is assumed as a frozen core. The Nijmegen soft-core potentials, NSC97e and NSC97f, were used for the valence baryon-baryon part, and the phenomenological potentials were employed for the $\alpha - B$ parts ($B=N, \Lambda, \Xi$ and Σ). In the two-baryon system ($\Lambda\Lambda$ - ΞN - $\Sigma\Sigma$) with 1S_0 and $I = 0$, we found that the NSC97e and NSC97f have a deeply bound state ($B_{\Lambda\Lambda} = 1500 \sim 1600$ MeV), whose character is of the flavor-SU(3)-{8s}-like and is similar to the Pauli-forbidden state in the quark-cluster model. Such a deeply bound state gives no effect to the low-energy scattering parameters of NSC97e (NSC97f), although the existence seems to be improper in the OBEP framework. We thus called it as a pseudo bound state and impose the following condition on the wave function of many baryon system when the NSC97 potentials are applied to many-body system: physical states should be orthogonal to the pseudo bound states. It was then found that the calculated $\Delta B_{\Lambda\Lambda}$ of ${}^6_{\Lambda\Lambda}\text{He}$ for NSC97e and NSC97f are, respectively, 0.6 and 0.4 MeV in the full coupled-channel calculation. The results are about half in comparison with the experimental data, $\Delta B_{\Lambda\Lambda}^{exp} = 1.01 \pm 0.20^{+0.18}_{-0.11}$ MeV.

In the present study, we neglected the Σ - Λ coupling effect, the importance of whose effect

has been recently pointed out in ${}^5_{\Lambda}\text{He}$ [27]. Since the ${}^5_{\Lambda}\text{He}$ nucleus is expected to be described with the extended α -cluster model, $[(3N + N) + \Lambda]$ and $[(3N + N) + \Sigma]$, we can study the Λ - Σ coupling effect in ${}^6_{\Lambda\Lambda}\text{He}$, if we use the $[(3N + N) + \Lambda + \Lambda] + [(3N + N) + \Xi + N] + [(3N + N) + \Sigma + \Sigma]$ model. The study will give a basic starting point for us to perform the systematic structure study taking into account the Λ - Σ coupling in p -shell double- Λ hypernuclei as well as the single- Λ hypernuclei. Such an approach is now planning and partially in progress.

Acknowledgments

We greatly acknowledge helpful discussions with E. Hiyama, M. Kamimura, T. Motoba, Th.A. Rijken, and Y. Yamamoto.

-
- [1] H. Takahashi *et al.*, Phys. Rev. Lett. **87**, 212502 (2001).
- [2] D.J. Prowse, Phys. Rev. Lett. **17**, 782 (1966).
- [3] I.N. Filikhin and A. Gal, Phys. Rev. C**65**, 041001 (R) (2002).
- [4] I.N. Filikhin and A. Gal, Nucl. Phys. **A707**, 491 (2002).
- [5] I.N. Filikhin, A. Gal, and V.M. Suslov, Phys. Rev. C **68**, 024002 (2003).
- [6] V.G.J. Stoks and Th.A. Rijken, Phys. Rev. C **59**, 3009 (1999).
- [7] E. Hiyama, M. Kamimura, T. Motoba, T. Yamada, and Y. Yamamoto, Phys. Rev. C **66**, 024007 (2002).
- [8] K.S. Myint, S. Shinmura, and Y. Akaishi, Eur. Phys. J. A. **16**, 21 (2003).
- [9] M. Kohno, Y. Fujiwara, and Y. Akaishi, Phys. Rev. C**68**, 034302 (2003).
- [10] I. Vidanã, A. Ramos and A. Polls, nucl-th/0307096, (2003).
- [11] D.E. Lanskoy and Y. Yamamoto, Phys. Rev. C **69**, 014303 (2004).
- [12] H. Nemura *et al.*, talked at the International Symposium on Hypernuclear and Strange Particle Physics (HYP03), (2003).
- [13] T. Yamada and C. Nakamoto, Phys. Rev. C **62**, 034319 (2000).
- [14] M. Kamimura, Phys. Rev. A **38**, 621 (1988).
- H. Kameyama, M. Kamimura, and Y. Fukushima, Phys. Rev. C **40**, 974 (1989).
- E. Hiyama, Y. Kino, and M. Kamimura, Prog. Part. Nucl. Phys. **51**, 1 (2003).
- [15] S. Saito, Prog. Theor. Phys. **41**, 705 (1969).
- [16] V.I. Kukulin, V.M. Krasnopol'sky, V.T. Voronchev, and P.B. Sazanov, Nucl. Phys. **A417**, 128 (1984).
- [17] Y. Yamamoto, T. Motoba, H. Himeno, K. Ikeda, and, S. Nagata, Prog. Theor. Phys. Suppl. **117**, 361 (1994).
- [18] T. Fukuda *et al.*, Phys. Rev. C **58**, 1306 (1998).
- [19] T. Nagae *et al.*, Phys. Rev. Lett. **80**, 1605 (1998).
- [20] For example, C.W. De Jager, H. De Vries, and C. De Vries, At. Data Nucl. Data Tables **14**, 480 (1974).
- [21] H. Kanada, T. Kanako, S. Nagata, and M. Nomoto, Prog. Theor. Phys. **61**, 1327 (1979).
- [22] Th.A. Rijken, private communication (2003).

- [23] P.M.M. Maessen, T.A. Rijken, and J.J. de Swart, *Phys. Rev. C* **40**, 2226 (1989).
- [24] M. Oka and K. Yazaki, in *Quarks and Nuclei*, edited by W. Wise (World Scientific, Singapore, 1984), p. 489.
- [25] H. Noumi et al., *Phys. Rev. Lett.* **89**, 072301 (2002).
- [26] A. Hasegawa and S. Nagata, *Prog. Theor. Phys.* **45**, 1786 (1971); Y. Yamamoto, *ibid.* **52**, 471 (1974).
- [27] H. Nemura, Y. Akaishi and Y. Suzuki, *Phys. Rev. Lett.* **89**, 142504 (2002).

TABLE I: Calculated energies ($E_{\Lambda\Lambda} = -B_{\Lambda\Lambda}$) and channel components of the 1S_0 state of two-baryon system with $S = -2$ and $I = 0$ for various coupled channel cases, where we use the NSC97e and NSC97f potentials with the momentum-dependent term.

NSC97e potential					
channel	state	$E_{\Lambda\Lambda}$ (MeV)	$P_{\Lambda\Lambda}$ (%)	$P_{\Xi N}$ (%)	$P_{\Sigma\Sigma}$ (%)
$\Lambda\Lambda$	0_1^+	1.18	100.0	–	–
$\Lambda\Lambda$ - ΞN	0_1^+	1.10	99.9	0.1	–
$\Lambda\Lambda$ - $\Sigma\Sigma$	0_1^+	-21.4	48.0	–	52.0
	0_2^+	1.40	99.7	–	0.3
ΞN - $\Sigma\Sigma$	0_1^+	4.41	–	31.2	68.8
	0_2^+	29.34	–	99.9	0.1
$\Lambda\Lambda$ - ΞN - $\Sigma\Sigma$	0_1^+	-1475	26.6	31.1	42.4
	0_2^+	1.15	100.0	0.0	0.0
NSC97f potential					
channel	state	$E_{\Lambda\Lambda}$ (MeV)	$P_{\Lambda\Lambda}$ (%)	$P_{\Xi N}$ (%)	$P_{\Sigma\Sigma}$ (%)
$\Lambda\Lambda$	0_1^+	1.19	100.0	–	–
$\Lambda\Lambda$ - ΞN	0_1^+	1.15	100.0	0.0	–
$\Lambda\Lambda$ - $\Sigma\Sigma$	0_1^+	1.08	99.9	–	0.1
ΞN - $\Sigma\Sigma$	0_1^+	-81.98	–	28.2	71.8
	0_2^+	29.31	–	100.0	0.0
$\Lambda\Lambda$ - ΞN - $\Sigma\Sigma$	0_1^+	-1624	23.9	32.1	44.0
	0_2^+	1.17	100.0	0.0	0.0

TABLE II: Calculated $\Delta B_{\Lambda\Lambda}$ and the channel components of ${}^6_{\Lambda\Lambda}\text{He}$ with (without) the exclusion operator V_{PBS} in Eq. (18), where the NSC97e and NSC97f potentials are used.

potential	channel	V_{PBS}	state	$\Delta B_{\Lambda\Lambda}$ (MeV)	$P_{\Lambda\Lambda}$ (%)	$P_{\Xi N}$ (%)	$P_{\Sigma\Sigma}$ (%)
NSC97e	$\Lambda\Lambda-\Xi N-\Sigma\Sigma$	<i>Yes</i>	0_1^+	0.61	99.77	0.21	0.01
	$\Lambda\Lambda$	<i>No</i>	0_1^+	0.33	100	–	–
	$\Lambda\Lambda-\Xi N$	<i>No</i>	0_1^+	1.36	99.45	0.55	–
	$\Lambda\Lambda-\Xi N-\Sigma\Sigma$	<i>No</i>	0_1^+	1467	26.65	30.97	42.38
	$\Lambda\Lambda-\Xi N-\Sigma\Sigma$	<i>No</i>	0_2^+	0.61	99.77	0.21	0.01
NSC97f	$\Lambda\Lambda-\Xi N-\Sigma\Sigma$	<i>Yes</i>	0_1^+	0.36	99.81	0.18	0.01
	$\Lambda\Lambda$	<i>No</i>	0_1^+	0.09	100	–	–
	$\Lambda\Lambda-\Xi N$	<i>No</i>	0_1^+	0.56	99.79	0.21	–
	$\Lambda\Lambda-\Xi N-\Sigma\Sigma$	<i>No</i>	0_1^+	1614	24.01	31.98	44.01
	$\Lambda\Lambda-\Xi N-\Sigma\Sigma$	<i>No</i>	0_2^+	0.36	99.81	0.18	0.01

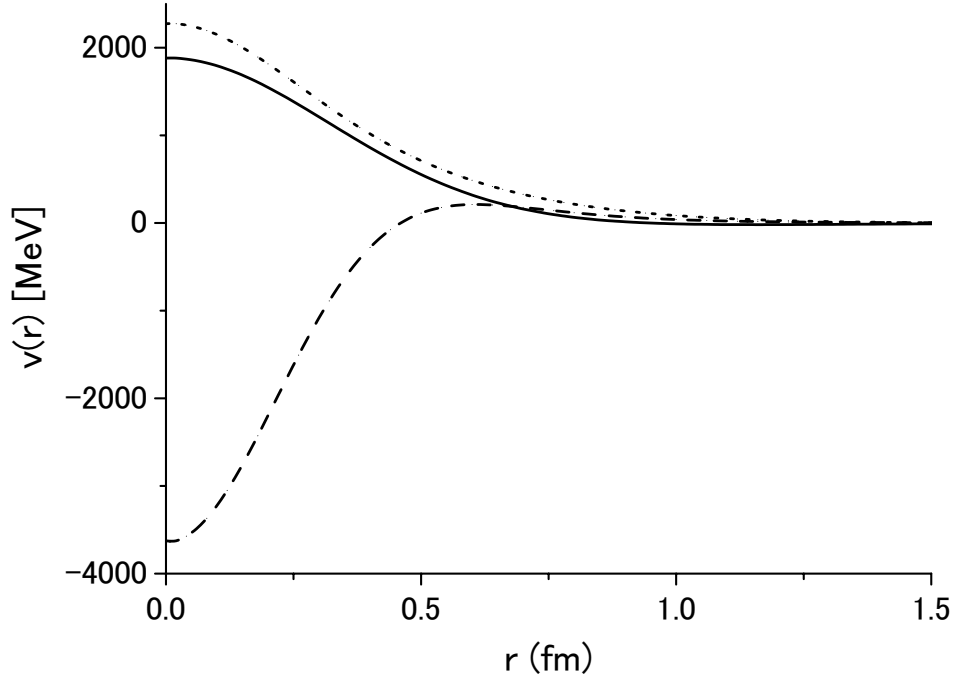


FIG. 1: Radial behavior of the bare potentials, $v_{\Lambda\Lambda-\Lambda\Lambda}(r)$ (solid line), $v_{\Xi N-\Xi N}(r)$ (dotted) and $v_{\Lambda\Lambda-\Xi N}(r)$ (dashed), for the NSC97e potential.

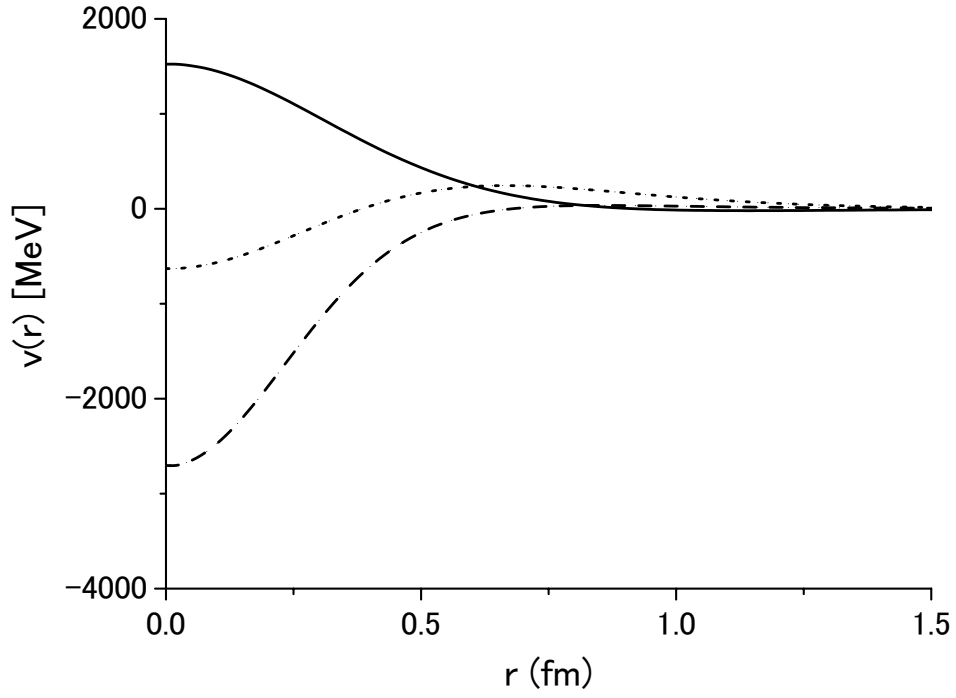


FIG. 2: Radial behavior of the bare potentials, $v_{\Lambda\Lambda-\Lambda\Lambda}(r)$ (solid line), $v_{\Sigma\Sigma-\Sigma\Sigma}(r)$ (dotted) and $v_{\Lambda\Lambda-\Sigma\Sigma}(r)$ (dashed), for the NSC97e potential.

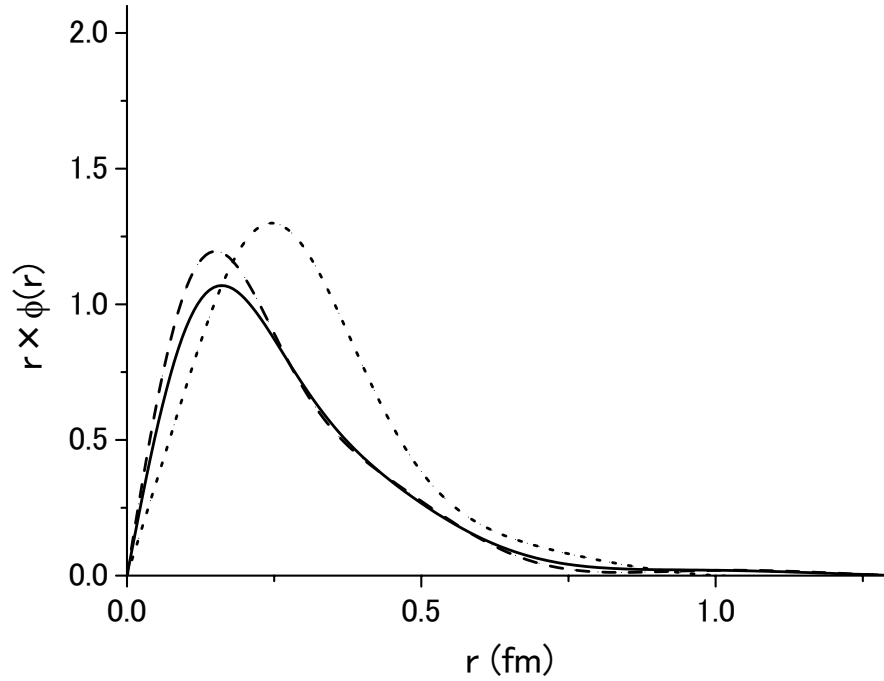


FIG. 3: Radial behavior of the relative wave function (multiplied to r) between the two baryons in the pseudo bound state with the flavor-SU(3)- $\{8s\}$ -like character, where we use the NSC97e potential with the momentum-dependent term. The solid, dashed and dotted lines denote the $\Lambda\Lambda$ -, ΞN - and $\Sigma\Sigma$ -channel wave functions, respectively.

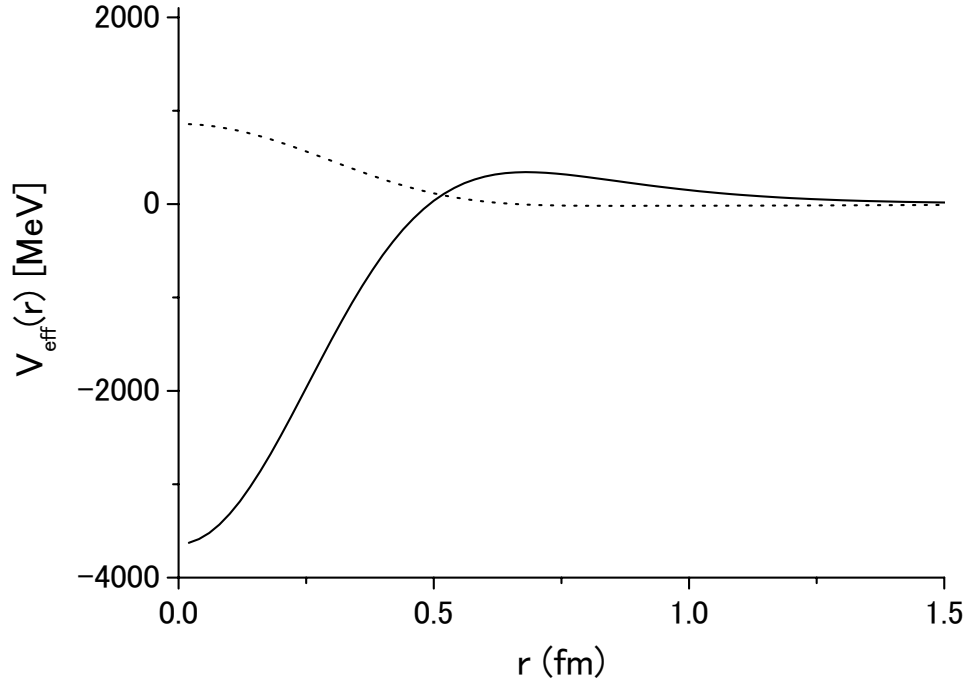


FIG. 4: Effective potentials for the flavor-SU(3) states (1S_0) with $S = -2$ and $I = 0$: $\{8s\}$ (solid line) and $\{27\}$ (dotted), where we use the NSC97e potential with the momentum-dependent term.